



Alprazolam-induced EEG spectral power changes in rhesus monkeys: a translational model for the evaluation of the behavioral effects of benzodiazepines

Lais F. Berro¹ · John S. Overton¹ · Jaren A. Reeves-Darby¹ · James K. Rowlett¹

Received: 9 August 2020 / Accepted: 4 February 2021 / Published online: 16 February 2021

© The Author(s), under exclusive licence to Springer-Verlag GmbH, DE part of Springer Nature 2021

Abstract

Rationale Benzodiazepines induce electroencephalography (EEG) changes in rodents and humans that are associated with distinct behavioral effects and have been proposed as quantitative biomarkers for GABA_A receptor modulation. Specifically, central EEG beta and occipital EEG delta activity have been associated with anxiolysis and sedation, respectively. The extent to which nonhuman primates show the same dose- and topography-dependent effects remained unknown.

Objectives We aimed at establishing a nonhuman primate model for the evaluation of benzodiazepine EEG pharmacology.

Methods Four adult male rhesus monkeys were prepared with fully implantable telemetry devices that monitored activity, peripheral body temperature, and contained two EEG (central and occipital), one electromyography (EMG), and one electrooculography channel. We investigated daytime alprazolam-induced changes in EEG spectral power, sleep–wake states, EMG activity, locomotor activity, and body temperature. Alprazolam (0.01–1.8 mg/kg, i.m.) or vehicle was administered acutely, and telemetry recording was conducted for 1 h.

Results Daytime alprazolam dose-dependently increased central EEG power (including beta activity), increased occipital EEG delta power, and decreased occipital EEG alpha, theta, and sigma power. There was an ~8-fold difference in the potency of alprazolam to increase central EEG beta vs. occipital EEG delta activity (based on relative EEG power). The highest dose, which increased both central EEG beta and occipital EEG delta relative power, induced sedative effects (increased time spent in N1 and N2 sleep stages) and decreased peripheral body temperature and locomotor activity.

Conclusions Alprazolam induces dose- and topography-dependent EEG changes in rhesus monkeys and provides a valuable model for studying benzodiazepine pharmacology.

Keywords Alprazolam · Benzodiazepine · EEG · Spectral power · Sedation · Rhesus monkey

Introduction

Benzodiazepines are among the most widely prescribed psychiatric drugs in the USA (Moore and Mattison 2017), with more than 1 in 20 people filling a benzodiazepine prescription each year (Bachhuber et al. 2016). The most recent data indicate that during 2014–2016, the rate of visits at which

benzodiazepines were prescribed in the USA was 27 annual visits per 100 adults (Santo et al. 2020). Although these drugs can be prescribed for several conditions, anxiety and mood disorders accounted for the majority of benzodiazepine prescriptions (Santo et al. 2020). In addition to a high rate of prescriptions, benzodiazepine misuse also has become a worldwide public health concern (Votaw et al. 2019), and the search for a benzodiazepine-type drug that retains therapeutic efficacy, yet shows reduced abuse liability and side effect profiles, continues to be of utmost importance for psychiatric medicine.

Benzodiazepines exert their pharmacological effects by binding to γ -aminobutyric acid type A (GABA_A) receptors (Möhler 2011), with their major targets being GABA_A receptors containing α 1, α 2, α 3, and α 5 subunits (α 1GABA_A, α 2GABA_A, α 3GABA_A, and α 5GABA_A, respectively; for reviews, see Engin et al. 2018; Möhler 2011). Through their

This article belongs to a Special Issue on Imaging for CNS drug development and biomarkers

✉ Lais F. Berro
lberro@umc.edu

¹ Department of Psychiatry and Human Behavior, University of Mississippi Medical Center, 2500 N State St, Jackson, MS 39216, USA

interaction with these receptors, benzodiazepines modulate cortical network oscillations, as reflected by a well-documented electroencephalography (EEG) signature (Leiser et al. 2011). Benzodiazepine drugs increase beta band EEG activity both in rodent models (Coenen and van Luijckelaar 1991; Jongsma et al. 2000; van Lier et al. 2004; Christian et al. 2015) and in humans (Saletu et al. 2006; Gilles and Luthringer 2007). This effect has been proposed as a quantitative biomarker for GABA_A receptor modulation (Visser et al. 2003) and has been associated with subject-rated decreases in both anxiety in healthy human volunteers and in generalized anxiety disorder (Buchsbaum et al. 1985).

While lower benzodiazepine doses are associated with anxiety-reducing effects, high doses have been associated with sedative effects. The EEG correlates of benzodiazepine-induced sedation also have been established and include increases in beta, sigma, and delta EEG activity (Schulte am Esch and Kochs 1990; Veselis et al. 1991; Hering et al. 1994; Liu et al. 1996; Schnider et al. 1996). In a drug-free state, beta and gamma band EEG power increases have been associated with increased arousal (Brown et al. 2012) and the execution of cognitive tasks (Tallon-Baudry et al. 2004; Christian et al. 2015). Therefore, the fact that benzodiazepine-induced sedation is accompanied by increased EEG beta and gamma power represents a paradox, which has long been referred to as “pharmacological dissociation” (Coenen and van Luijckelaar 1991).

Benzodiazepine-induced changes in EEG power spectrum seem to follow a topographic distribution. Buchsbaum et al. (1985) have shown increases in beta activity in central and parietal brain regions with anxiolytic doses of clorazepate in patients with generalized anxiety disorder. Nishida et al. (2016) also showed increased beta and sigma EEG activities and decreased theta activity in central brain regions with sedative doses of the benzodiazepine midazolam. Moreover, midazolam has been shown to increase EEG beta power and decrease EEG alpha power during wakefulness, with beta power changes being most pronounced in frontal and central derivations and alpha power changes being most pronounced in the occipital position (Veselis et al. 1991). Finally, Nutt et al. (2015) demonstrated that the administration of the benzodiazepine-type drug zolpidem increased EEG beta band frequency in central brain regions and EEG delta band frequency in occipital brain regions in healthy volunteers. These studies indicate the importance of multi-lead recording in assessing EEG correlates of benzodiazepine action, particularly recordings including central and occipital EEG derivations.

An important feature of EEG pharmacology is that changes in EEG spectral power induced by benzodiazepines represent a highly translatable biomarker, being observed in rodents (e.g. Christian et al. 2015) and humans (e.g. Nutt et al. 2015). Therefore, the use of EEG for the evaluation of benzodiazepine effects has allowed researchers to complement commonly used behavioral assessments, which often lack face and

construct validity. However, the extent to which other species, particularly highly translational species such as nonhuman primates, show the same dose- and topography-dependent pattern of effects on EEG power spectrum with benzodiazepine treatment remained unknown. In the present study, we aimed at establishing a nonhuman primate model for the evaluation of benzodiazepine EEG pharmacology. Critically, our primate species used, rhesus macaques, have been shown recently to share GABA_A receptor subtype distributions in the brain that align with human findings, but not similar findings with rodent species (Sperk et al. 2020). Rhesus monkeys were prepared with fully implantable telemetry devices which continuously monitored activity and body temperature, in addition to containing two EEG channels (central and occipital), one electromyography (EMG) channel and one electrooculography (EOG) channel. We investigated alprazolam-induced EEG spectral power and sleep–wake state changes during the light (active) phase, as well as the effects of alprazolam on EMG, daytime activity, and body temperature. Based on the human literature, we expected that alprazolam treatment would increase EEG beta and sigma power in the central EEG derivation, while EEG delta power would be increased and EEG alpha power would be decreased in the occipital EEG derivation following alprazolam treatment.

Material and methods

Subjects

Four adult (ages 9–15) male rhesus monkeys (*Macaca mulatta*) weighing 12–16 kg were housed individually, but had visual, auditory, and olfactory contact with other monkeys throughout the study, as well as access to chew toys and a mirror in their cage. Subjects were maintained on a 12-h light/12-h dark cycle (lights on at 6 a.m., defined as Zeitgeber Time 0—ZT0), at a temperature of 21 ± 2 °C, with water available *ad libitum* and monkey diet available once/day, supplemented by fresh fruit and forage (seeds and dry fruit), and were weighed monthly during physical examinations. Amount of chow for each monkey was determined in consultation with veterinary staff to be that which maintains healthy weights in rhesus monkeys. Animals were fed in the afternoon, and experimental sessions were conducted in the mornings. All four subjects were experimentally naïve prior to the beginning of the studies. The monkeys were prepared with a telemetry implant according to the surgical procedures described below at least 1 month prior to the beginning of tests. All of the procedures and animal maintenance were in accordance with the Guide for the Care and Use of Laboratory Animals (National Research Council 2011), with review and approval via the Institutional Animal Care and Use Committees of the University of Mississippi Medical Center.

Surgical procedures

Animals were fully anesthetized with ketamine (10 mg/kg, i.m.) and atropine (0.05 mg/kg, i.m.), and anesthesia was maintained throughout the procedure with inhaled isoflurane (1–2%). Aseptic preparation of the surgical site (dorsum, head, neck, and around either the right or left eye) occurred in the prep room. Hair was removed using clippers, and the surgical site was prepared with three alternating applications of surgical scrub (chlorhexidine) and 70% alcohol. After preparation, animals were placed on the surgical table in sternal recumbency with access to the dorsum and head using patient positioning devices (Versa Form positioning pillow, Performance Health, IL, USA). Additional towels/pads were used to support the animal as needed. Arms were positioned, so the neck area was not tense or bunched, either back or out to the sides. The animal was positioned in such a way—ventral recumbency, with the head elevated—that the implant and all leads (electroencephalography [EEG], electromyography [EMG], and electrooculography [EOG]) could be placed without having to reposition the animal. Sterile corner drapes were placed over each ear and the face, and sterile drapes were placed on the entire animal. Drapes were stapled down to the skin using surgical skin staplers to create defined working area on head.

The telemetry device (Model L04 PhysioTel™ Digital; Data Sciences International® [DSI], St. Paul, MN, USA) consisted of an implant device (implant weight: 56 g; implant volume: 29 cc; implant dimensions: 59 × 38 × 15 mm) attached to a small antenna and to eight leads, two for each biopotential channel (four channels total). These implants were chosen because they consist of a fully implantable wireless telemetry system that allowed for simultaneous recording of EEG/EMG/EOG, activity, and temperature without the need for a head mount or a head cap. With these devices, all electrodes are implanted subcutaneously, and therefore, once animals recover from surgeries, there is significantly reduced potential for complications, and animals can move freely in their home cages. For the device implantation, a skin incision was made lateral to the spine beginning just caudal to the scapulae and extending caudally. The device was placed under the latissimus dorsi muscle, and the pocket size was increased as needed by blunt dissection to accommodate the device. The surgeon then visualized approximately how far caudally the antenna would extend, and a small stab incision was made slightly distal to that point. A trocar and cannula were passed between the main implant pocket and the stab incision, and the cannula was used to guide the antenna in a straight path distally. Non-absorbable suture (3-0 non-absorbable Prolene; Ethicon, NJ, USA) was used to tack the device to the underlying fascia.

A new incision was then made, beginning caudal to the brow bone and extending to approximately the inion. A trocar and cannula were used to tunnel the biopotential leads from

the dorsal pocket (implant placement site) to the cranial incision. Leads (EEG/EMG/EOG) were routed together. A small loop of lead was left at the dorsal pocket (implant placement site), and the incision was packed with moistened gauze. Some excess lead length was left to provide strain relief and prevent the leads from being pulled out of place with normal postural changes and activity.

Four EEG leads (2 channels, 2 leads each) were placed in the skull, one in a central derivation (C4–Cz) and the other in an occipital derivation (O2–Oz). Scalp electrode placement was based on the human 10–20 System of Electrode Placement. For the placement of the EEG leads, all muscle, connective tissue, and periosteum covering the skull was reflected with periosteal elevators, and Gelpi retractors were inserted at the rostral and caudal aspects of the incision. Measurements were made on skull with sterile tape measure, and insertion sites were marked with sterile marker. The leads were then prepared by trimming the leads to an appropriate length, exposing the wire lead by making a circumferential cut to remove the silicone insulation covering off the distal 3–5 cm of the lead. A piece of non-absorbable suture (4-0 non-absorbable Prolene; Ethicon, NJ, USA) was tied around the distal-most portion of the insulation to help prevent it from slipping back and fluid migration. The exposed wire was bent into a small loop and secured with a mosquito hemostat, and a stainless steel self-tapping round-head screw (part number 0–80 × 3/16, size 0-80, shaft length 4.8 mm, head diameter 2.5 mm, shaft diameter 1.57 mm, Plastic One, VA, USA) was placed inside the loop. If the head of the screw fits through the loop, the loop was made tighter. Another piece of non-absorbable suture (4-0 non-absorbable Prolene; Ethicon, NJ, USA) was tied around the loop to secure it. A drill was then placed firmly against the skull at a perpendicular angle, and the skull was perforated in the desired locations (C4, Cz, O2, and Oz). The holes were made so they passed completely through the bone, but did not perforate the dura to allow for supradural recording. Lavage with saline was performed the entire time drill was in use. As the screws were tightened down, a loop of lead was created on the surface of the skull around the screw to provide strain relief. Any excess wire from the loop was trimmed, and the skull was etched with scalpel blade around the screws before placing the dental acrylic. All exposed wire and screw was covered with dental acrylic, and dental acrylic (Maxcem Elite™, Kerr Corporation, CA, USA) was smoothed, and lead material was pushed down against the surface of the skull. A UV cure light (Maxima 2000 LED Curing Light Cordless Complete Unit, Henry Schein, NY, USA) was shown on the acrylic at least two times to induce hardening.

For the placement of the EMG leads (one channel, two leads), the cranial skin incision was extended as needed, ~4 cm, to expose the longitudinal muscle of the neck (trapezius). An area of the muscle that could accommodate lead

attachment and allow the leads to lie flat under the skin was selected. The leads were cut to an appropriate length, leaving some excess to allow for postural changes. The wire lead was exposed by making a circumferential cut to remove the silicone insulation covering off the distal 5–6 mm of the lead. A piece of non-absorbable suture (4-0 non-absorbable Prolene; Ethicon, NJ, USA) was tied around the distal-most portion of the insulation to help prevent it from slipping back and fluid migration. Approximately 4 mm of muscle tissue was tunneled through perpendicular to the long axis of the fiber bundles using an 18-gauge needle. The needle passed from the outer margins of the animal toward the midline. The exposed lead wire was passed into the lumen of the needle so that, as the needle is withdrawn, most of the wire was left embedded in the muscle. Approximately 1 cm of the distal end of the wire was exteriorized from the muscle. Insulation was placed onto the terminal end of the lead wire, secured with a non-absorbable suture tie (4-0 non-absorbable Prolene; Ethicon, NJ, USA) and trimmed to length so that the insulation extended slightly beyond the wire. This anchored the lead in place and protected the animal's skin from the cut end of the wire. The process was repeated for the other leads. Leads were placed approximately 4 mm apart within the same group of muscle fibers, ensuring that the exposed wire from the leads did not make contact as that could cause shorting of the signal.

For the placement of the EOG leads (one channel, two leads), the leads were routed subcutaneously from the head incision to the eye orbit (right eye for two subjects, left eye for the other two subjects), exiting the eye orbit from underneath the upper eyelid. No incision was made for the placement of the EOG leads. Once the leads had been externalized, the wire lead was exposed by making a circumferential cut to remove the silicone insulation covering off the distal 5–6 mm of the lead. A piece of non-absorbable suture (4-0 non-absorbable Prolene; Ethicon, NJ, USA) was tied around the distal-most portion of the insulation to help prevent it from slipping back and fluid migration. The periosteum of the orbit was then elevated, and the exposed wire and lead were affixed to and under the periosteum with non-absorbable suture (4-0 non-absorbable Prolene; Ethicon, NJ, USA) in a simple interrupted pattern. One lead was affixed at a position adjacent to the lateral canthus of the eye, and the other lead was affixed at a position adjacent to the medial canthus of the eye. The exposed wire was completely covered with periosteum and a small portion of conjunctiva.

Once all leads were placed and secured, the animal's dorsal incision (implant placement site) was sutured in two layers. The subcutaneous layer was sutured with absorbable suture (4-0 absorbable Vicryl on taper; Ethicon, NJ, USA) in a simple continuous pattern. Skin was then closed with an intradermal pattern using absorbable suture (4-0 absorbable Vicryl on cutting; Ethicon, NJ, USA). Stab incision (antenna placement site) was closed by suturing the skin layer, as described above.

The muscle layer on the head incision was sutured using a combination of interrupted tension-relieving suture patterns (3-0 absorbable Biosyn on taper; Ethicon, NJ, USA) and a simple continuous pattern (4-0 absorbable Vicryl on taper; Ethicon, NJ, USA). Subcutaneous tissue was then closed in a simple continuous pattern with absorbable suture (4-0 absorbable Biosyn on taper; Ethicon, NJ, USA). Skin was then closed with an intradermal pattern using absorbable suture (4-0 absorbable Vicryl on cutting; Ethicon, NJ, USA).

All animals received pre-operative steroids (dexamethasone, 1–2 mg/kg, i.m.) and analgesics (buprenorphine SR, 0.045 mg/kg, s.c.), perioperative anesthetic monitoring, and post-operative analgesics (carprofen 4 mg/kg, p.o.) for 7 days and antibiotics (cephalexin, 20 mg/kg, p.o.) for 7 days and were allowed a minimum of 1-month recovery period before experiments.

Experimental design and dosing procedures

In order for telemetry implants to be turned on, the area on the animal's back in which the telemetry device was implanted required touching by a magnet while the receivers located inside the room were actively communicating with a computer located outside of the room. Therefore, before the beginning of experiments, animals were trained with positive reinforcement techniques to present and were touched on their back/dorso (telemetry device implant site). All recordings were conducted in the animals' home cages.

The acute effects of daytime administration of alprazolam (0.01, 0.03, 0.1, 0.3, 1.0, and 1.8 mg/kg, i.m.) and vehicle (80% propylene glycol, 20% sterile H₂O) on EEG, EMG, activity, and body temperature were assessed during the light phase. Like most benzodiazepines, alprazolam is difficult to get and stay in solution; therefore, water was used instead of saline, and drug solutions were mixed immediately before injections. Doses of alprazolam were chosen based on previous studies from our laboratory investigating the anxiolytic-related effects of intravenous alprazolam in rhesus monkeys using a conflict procedure (average ED₅₀ [mg/kg, i.v., (95% CI)] for four rhesus monkeys = 0.007 mg/kg; Rowlett et al. 2006). Telemetry implants were turned on at least 15 min prior to injections by touching the telemetry device implant site on the animal's back with a magnet. Animals were administered an intramuscular injection of drug or vehicle at around 4ZT (injection time recorded for each individual subject), and telemetry recording continued for a period of at least 2 h. Mid-morning was chosen for our recordings to mimic the time of day when patients frequently take benzodiazepines for anxiolytic purposes and also to control for circadian and homeostatic pressure. Test sessions were performed on Mondays and Thursdays, allowing for a 2-day washout period to elapse between each treatment. A baseline recording was conducted both before and after the end of the test sessions at the same

period (4ZT–6ZT), and baseline data for each monkey consist of an average of the two baseline recording sessions. The order of tests (including drug doses and vehicle) was randomized and counterbalanced across subjects.

Electrophysiological, daytime activity, and body temperature recording

Two telemetry receivers (TRX-1; DSI, St. Paul, MN) were mounted inside the room where animals were housed to allow for real-time EEG/EMG, activity and body temperature recording. Continuous acquisition of the EEG, EMG, activity, and temperature telemetry signals occurred using the Ponemah physiologic data acquisition software (version 6.41; DSI, St. Paul, MN); the frequency range of the L04 telemetry transmitters was 0.5–100 Hz for EEG/EMG channels. Body temperature (Celsius per second) and daytime activity (counts per second) data were collected through the L04 implant. The body temperature and daytime activity measures were averaged across 5-s intervals.

Sleep–wake state analysis

Sleep–wake states were determined by visual inspection of EEG, EMG, and EOG signals using NeuroScore software (version 3.2.0; DSI, St. Paul, MN) according to the American Academy of Sleep Medicine (AASM) guidelines for adult human sleep scoring (Manual version 2.5; Berry et al. 2018). Sleep–wake state scoring was conducted based on recordings from the central derivation (C4–Cz). Recordings from leads placed centrally reflect EEG activity summed from both frontal and parietal regions and are considered the most sensitive for recording sleep-related activity, with a single central derivation not differing from the AASM-recommended EEG derivations in terms of scoring reliability (Ruehland et al. 2011). Trained investigators classified each 30-s epoch as one of five states: WAKE, non-rapid eye movement (NREM) sleep stages N1, N2, or N3, or rapid eye movement (REM) sleep. WAKE was scored when > 50% of the epoch consisted of alpha (8–13 Hz) activity or low amplitude, mixed frequency (2–7 Hz) activity and active EMG, possibly accompanied by EOG reflecting rapid eye movements and/or rapid eye blinks. N1 (Stage 1) was scored when 50% of the epoch consisted of relatively low amplitude, mixed frequency (2–7 Hz) activity and < 50% of the epoch contained alpha (8–13 Hz) activity accompanied with lower EMG activity, and possible presence of slow eye movements. N2 (Stage 2) was scored when K-complexes (1–2-Hz isolated waves) and/or sleep spindles (regular 12–16-Hz EEG sequences) were observed and < 20% of the epoch contained high-amplitude (> 75 μ V), low-frequency (1–4 Hz) activity. N3 was scored when \geq 20% of the epoch consisted of high-amplitude (> 75 μ V), low-frequency (1–4 Hz) EEG waves (i.e., slow wave

activity). REM was scored when the epoch contained relatively low voltage, mixed frequency activity with predominant theta activity (4–8 Hz) accompanied with low EMG activity (i.e., atonia) and EOG showing rapid eye movements. Epochs with prominent artifacts were identified and excluded from subsequent EEG spectral analysis as described below.

Electroencephalography spectral analysis

Spectral analysis of EEG data was calculated using a Fast Fourier transform algorithm (NeuroScore, version 3.2.0; DSI, St. Paul, MN) on all epochs without artifacts. Fourier analysis was limited to frequencies < 100 Hz due to the frequency bandwidth of the L04 transmitters. Each 30-s epoch was visually screened for artifacts, and epochs with artifacts were removed from further analysis. The remaining data were analyzed, and spectral analysis was performed on 5-s epochs with a frequency resolution of 0.5 Hz. Contiguous frequencies were binned into standard frequency bands (delta: 0.3–4 Hz; theta: 4–8 Hz; alpha: 8–12 Hz; sigma: 12–16 Hz; beta: 16–30 Hz) as previously described in studies with nonhuman primates (Goonawardena et al. 2018), and the relative (percentage) power for each band was calculated.

Three dependent measures were evaluated: raw EEG power (referred to as “power” in μ V²/Hz), raw EEG power for an experimental condition compared to baseline raw EEG power (“normalized power”), and raw EEG power in each separate band as a percentage of the absolute power summed over the five frequency bands for each 5-s epoch, normalized to baseline relative power (“normalized relative power”).

Data analysis

Before the beginning of this study, power analyses were conducted (effect sizes were calculated as generalized eta-squared, η G2; Algina and Olejnik 2003; Bakeman 2005) using preliminary and published studies with $N = 5$ monkeys (Hsieh et al. 2008) and $N = 6$ monkeys (Authier et al. 2014, note this study used cynomolgus macaques). Based on these estimates, we were expected to obtain sufficient power (η G2 = 0.5, Bakeman 2005) with a sample size of $N = 4$. Because the designs of the previous studies were not based on evaluating a relatively broad range of doses of a drug for daytime EEG analyses, the power estimate is restricted to between-subjects generalization only.

No significant differences in EEG spectral analysis were observed during the second hour of recording compared to vehicle (data not shown). Therefore, all data were analyzed for the first hour of recording (starting at the moment of injection). Sleep stages are presented as the total time (in minutes) spent in each specific stage during the 1-h recording after scoring in 30-s epochs. EEG spectral power is presented for each EEG derivation (central vs. occipital) as the relative

(percentage) power for each band for each 5-s epoch. EMG, body temperature, and daytime activity data were averaged across 5-s intervals for the duration of the recording. Except for sleep–wake state data, all data were normalized as percentage of baseline.

All statistics were conducted with GraphPad Prism (release 7.02). For sleep–wake states analyses, the parameters (total sleep time, sleep latency, and time spent in N1, N2, and N3) were expressed as minutes out of a total of 60. These data were analyzed by separate repeated measures ANOVA and planned Dunnett's tests comparing vehicle to the three selected conditions: baseline, 0.3, and 1.8 mg/kg alprazolam.

Individual frequency bands in both derivations were analyzed for effect of alprazolam dose using trend analysis, via repeated measures analysis of variance (ANOVA). If a linear trend was detected (i.e., slope significantly different from zero), a pharmacologically defined potency (dose engendering 50% of maximum effect, ED_{50}) was analyzed using a 4-parameter logistic equation to iteratively fit each dose–response function. For this analysis, the minimal effect was constrained to baseline (100%), assuming a dose-dependent change from the baseline defining the effect. Note that this assumes a mono-directional effect, i.e., either an increase or decrease from baseline, which is an untested assumption. Because a key hypothesis of this study was that alprazolam-induced beta frequency increases occur at lower doses than alprazolam-induced delta-frequency increases, an F test was performed for beta vs. delta frequencies, first by comparing slopes, and if slopes were not significantly different, then by comparing the ED_{50} values.

The telemetry system obtained other data relevant for benzodiazepine pharmacology, including body temperature (peripheral), activity, and EMG. As with the EEG data, each measure was converted to percentage of baseline levels over the first 60 min following the injection, allowing comparisons with the EEG results. For all measures, repeated measures ANOVA were conducted with specific comparisons of each dose vs. vehicle (Dunnett's procedure). Because family-wise error rate was controlled for the Dunnett's tests, the comparisons were made to supplement ANOVA results and were conducted irrespective of the ANOVA results (Myers et al. 2010). For significant effects, we computed ED_{50} values as described above. In addition, we compared the effects of all doses of alprazolam for each power band with the three behavioral/physiological effects using a Pearson R correlation, in order to determine if any relationships were evident between power bands and other pharmacological effects of alprazolam. For all tests conducted in this study, the family-wise error rate was constrained to $p \leq 0.05$, and p values were reported up to four significant digits.

Drugs

Alprazolam was purchased commercially (Sigma-Aldrich, MO, USA) and was dissolved in 100% propylene glycol and diluted in water. Final solutions were prepared using 50–80% propylene glycol and 20–50% sterile water. Solutions were prepared immediately before injections, and all injections were administered intramuscularly. Propylene glycol may cause lesions if given intramuscularly at high concentrations/volumes. Therefore, for each dose, we used the highest concentration of drug and smallest amount of propylene glycol/injection volume possible that still maintained the drug in solution (injection volume varied between 0.01 and 0.04 ml/kg). Vehicle injections were given at the highest concentration of propylene glycol (80% propylene glycol and 20% sterile water) at the highest injection volume administered for that concentration (0.04 ml/kg).

Results

Sleep–wake state analysis

Sleep–wake state analysis is summarized in Fig. 1 (note that REM sleep was not detected for any of the test conditions, so these data are not shown). The top two panels show EEG/EMG/EOG determinations of total minutes sleeping (total sleep time) and the latency to initiate sleep, in minutes (sleep latency). For total sleep time, the ANOVA showed a significant treatment effect ($F_{3,9} = 60.65$, $p = 0.0007$), whereas for sleep latency the overall ANOVA was not significant ($F_{3,9} = 5.96$, $p = 0.06$). For both measures, the planned Dunnett's tests showed that the 1.8 mg/kg dose of alprazolam differed significantly from vehicle treatment ($p = 0.0037$ and $p = 0.017$, respectively), with total sleep time increased and sleep latency correspondingly decreased relative to vehicle. Vehicle was not significantly different from baseline for any measure (Dunnett's t tests).

Total time spent in each sleep stage is shown in the bottom graphs of Fig. 1. NREM stage N1 showed a modest increase relative to vehicle treatment (left bottom panel; $F_{3,9} = 6.86$, $p = 0.06$; 1.8 mg/kg significantly higher than vehicle, Dunnett's test, $p = 0.0357$). In contrast, most of the 60-min period that was recorded as sleep (~75%) consisted of stage N2 (right center panel; $F_{3,9} = 52.4$, $p = 0.0003$; 1.8 mg/kg significantly higher than vehicle, Dunnett's test, $p = 0.0068$). Finally, no significant differences due to treatment were observed for deep/slow-wave sleep (N3) (right bottom panel, $F_{3,9} = 3.00$, $p = 0.18$; no differences with Dunnett's tests), although individual monkeys showed very slight (i.e., 2 min or less) increases in N3 scoring with the highest dose of alprazolam. As with overall scores, vehicle was not significantly different from baseline for any of the sleep stage measures (Dunnett's t tests).

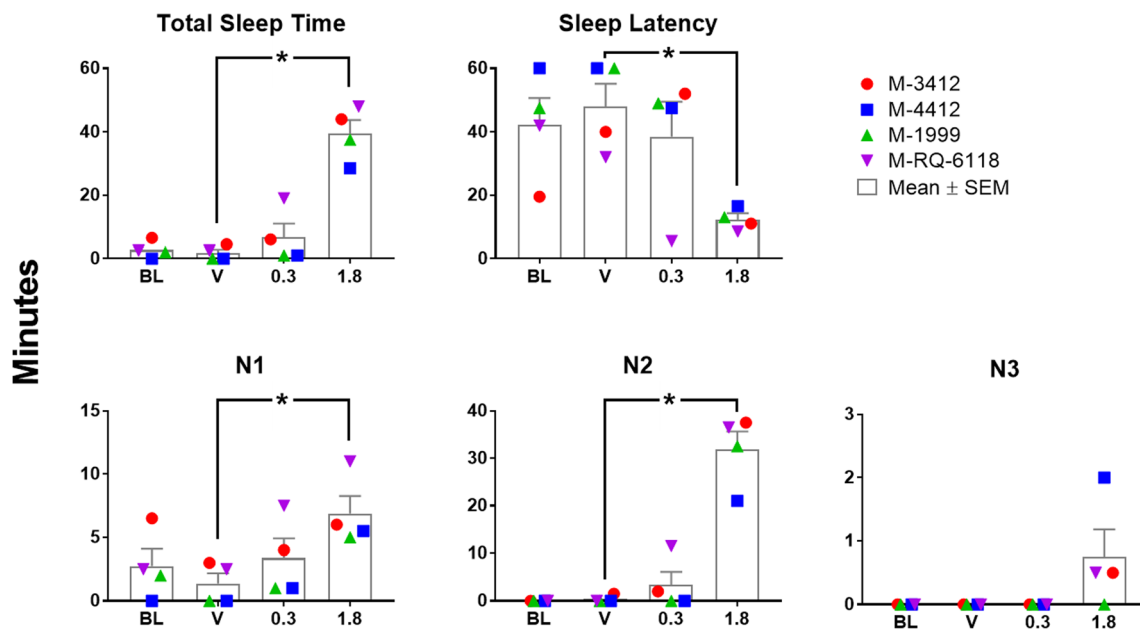


Fig. 1 Sleep–wake state analysis of selected doses of alprazolam after daytime administration in rhesus macaques. Sleep analysis was conducted with the central derivation following the first hour after i.p. injection of vehicle (V), 0.3 mg/kg alprazolam (a dose below the ED_{50} for beta band increases, see Fig. 2), and 1.8 mg/kg alprazolam (the highest

dose tested). Data are from individual monkeys (individual colored symbols) and mean + SEM (bars with error bars). A 1-h period of scoring with no injection and at approximately the same time as the alprazolam treatments served as baseline (BL). Note that $*p < 0.05$ vs. vehicle, Dunnett's test

Electroencephalography spectral analysis

The three frequency band measures for central and occipital derivations are shown in Fig. 2, with each plot representing vehicle or a dose of alprazolam (only the highest four doses shown for clarity). For the central derivations (Fig. 2, top three panels), frequency bands were increased with all three measures, although the significant increases for specific power bands depended on the measure. For the power data (Fig. 2, top left panel), all frequency bands were increased significantly except alpha (linear trend analyses: delta, $F_{1,18} = 4.864$, $p = 0.0407$; theta, $F_{1,18} = 6.122$, $p = 0.0235$; sigma, $F_{1,18} = 13.10$, $p = 0.002$; beta, $F_{1,18} = 37.74$, $p < 0.0001$). For the normalized power data (Fig. 2, top middle panel), all frequency bands were increased significantly (delta, $F_{1,18} = 6.693$, $p = 0.0186$; theta, $F_{1,18} = 26.40$, $p < 0.0001$; alpha, $F_{1,18} = 29.45$, $p < 0.0001$; sigma, $F_{1,18} = 23.60$, $p = 0.0001$; beta, $F_{1,18} = 45.21$, $p < 0.0001$). For normalized relative power (Fig. 2, top right panel), frequency bands were increased by alprazolam for beta and sigma frequencies only ($F_{1,18} = 40.95$ and 6.54 , $p < 0.0001$ and $p = 0.0198$, respectively).

For the occipital derivation (Fig. 2, bottom panels), overall both increases and decreases in frequency bands were found. For the power data (Fig. 2, bottom left panel), the delta frequency bands were higher for alprazolam doses than vehicle (linear trend analyses: $F_{1,18} = 4.442$, $p = 0.0493$) but decreased for theta ($F_{1,18} = 29.77$, $p < 0.0001$), sigma ($F_{1,18} = 135.6$, $p < 0.0001$), and beta ($F_{1,18} = 35.46$, $p < 0.0001$). For the normalized power data (Fig. 2, bottom middle panel), all

frequency bands except delta were decreased significantly (theta, $F_{1,18} = 36.64$, $p < 0.0001$; alpha, $F_{1,18} = 303.8$, $p < 0.0001$; sigma, $F_{1,18} = 207.0$, $p < 0.0001$; beta, $F_{1,18} = 37.66$, $p < 0.0001$). For normalized relative power (Fig. 2, bottom right panel), a significant increasing trend was observed for delta bands ($F_{1,18} = 27.87$, $p < 0.0001$), whereas significant decreasing trends were observed for theta ($F_{1,18} = 84.11$, $p < 0.0001$), alpha ($F_{1,18} = 35.74$, $p < 0.0001$), and sigma ($F_{1,18} = 29.14$, $p < 0.0001$) frequencies.

In order to compare potencies of frequency band changes, we used non-linear regression analysis to compute ED_{50} values for alprazolam at each frequency that showed a significant trend (Table 1). For this analysis, we used the normalized relative power only because these data were based on a proportion of a whole (total power) that resulted in maximum values that were relatively constant across frequency bands, i.e., ~150% for increases above baseline and ~60% for decreases below baseline (cf. Fig. 2, right top and bottom panels). Iterative fitting to the 4-parameter logistic equation resulted in R^2 values close to 1.0, except for the sigma band in the central derivation, which converged only after constraining the slope to 1.0. As can be seen in the table, the lowest alprazolam ED_{50} values were 0.037 and 0.038 mg/kg for alpha and theta band decreases in the occipital derivation, followed by 0.055 mg/kg for the expected beta band increase in the central derivation. Higher doses of alprazolam decreased sigma bands in occipital, and at approximately 10-fold higher doses than those that altered alpha, theta, and beta bands, the expected delta

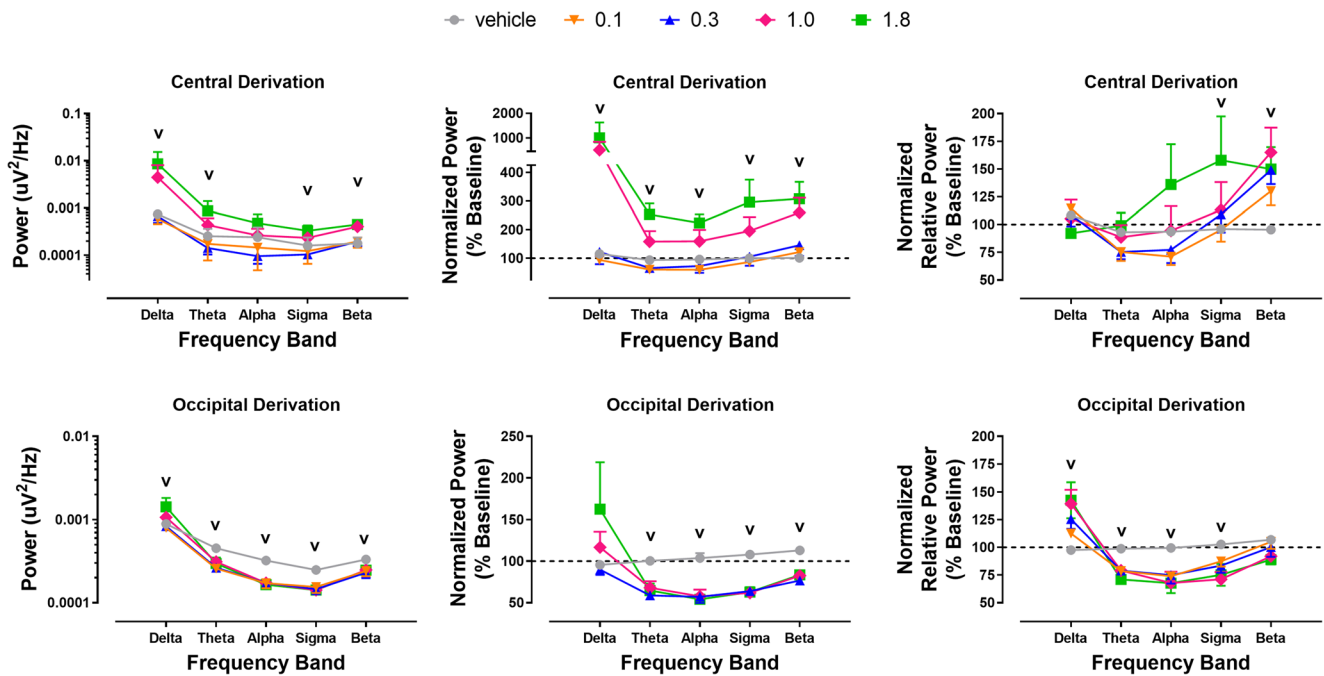


Fig. 2 Effects of alprazolam on frequency bands in central and occipital derivations. For clarity, only the four highest doses are shown. Left panel illustrates raw EEG power (referred to as “power” in $\mu\text{V}^2/\text{Hz}$, on a logarithmic scale). Middle panel illustrates normalized power, which is the raw EEG power for an experimental condition compared to baseline raw EEG power. Right panel illustrated normalized relative power or raw EEG power in each separate band as a percentage of the absolute power

summed over the five frequency bands for each 5-s epoch, normalized to baseline relative power. Top panels show the three measures for the central EEG derivation, and bottom panels show the same measures for the occipital EEG derivation. All data are shown as mean + SEM ($N = 4$). Each bandwidth was analyzed with a linear trend model (repeated measures ANOVA), significant trends are indicated by the “V” symbol

band increase was evident in the occipital derivation. The least potent effect was the sigma band increase in the central derivation at an ED_{50} of 1.1 mg/kg.

To the extent that beta band increases are associated with anxiolysis, whereas delta band effects are associated with sedation, one prediction for this study was that there would be a potency difference between these two frequency band increases. To evaluate this hypothesis, we used an F test to compare the slopes and ED_{50} values for central beta band vs. occipital delta band increases (Fig. 3, Table 1). The F test for slope showed no significant differences, suggesting similar

functions and allowing an unambiguous comparison of the ED_{50} values. These values were significantly different ($F_{1,8} = 22.6, p = 0.0014$), indicating an ~8-fold difference in the potency of alprazolam to increase central beta band frequencies vs. occipital delta band frequencies.

Peripheral body temperature, activity, and electromyography

As seen in Fig. 4 (top panel), alprazolam dose-dependently attenuated peripheral body temperature ($F_{6,18} = 10.25, p =$

Table 1 Non-linear regression analyses for potencies of each power band (normalized relative power, % baseline) following alprazolam administration in rhesus monkeys ($N = 4$).

Power band/derivation	Effect vs. baseline	ED_{50} , (mg/kg)	SEM	Goodness-of-fit (R^2)	Slope	SEM
Alpha/occipital	Decrease	0.037	0.0078	0.95	1.2	0.28
Theta/occipital	Decrease	0.038	0.017	0.85	0.48	0.13
Beta/central	Increase	0.055	0.022	0.86	0.75	0.23
Sigma/occipital	Decrease	0.22	0.072	0.92	0.95	0.27
Delta/occipital	Increase	0.45	0.078	0.97	0.68	0.022
Sigma/central	Increase	1.1	0.68	0.69	1.0*	NA

Dose–response functions were fit according to the 4-parameter logistic equation, with the minimal effect constrained to 100, except *Sigma/central, in which the slope also was constrained to 1.0 in order to obtain a significant fit

Abbreviation: NA, not applicable due to constraint

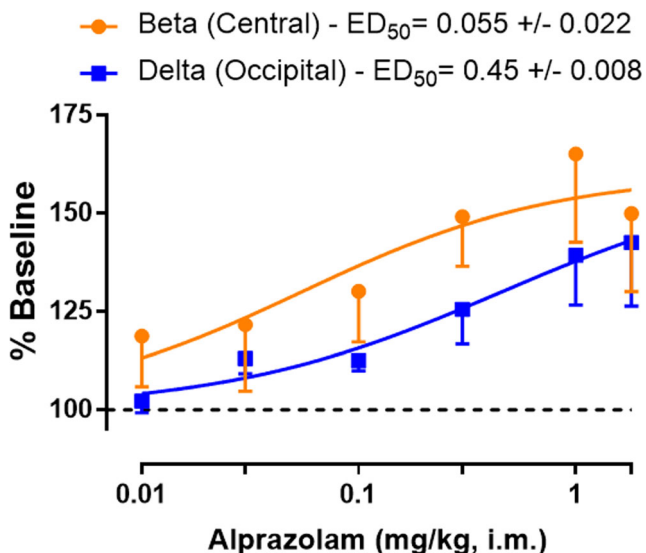


Fig. 3 Comparison of non-linear regression functions for alprazolam-induced increases in beta frequency bands (central derivation) and delta frequency bands (occipital derivation) in rhesus monkeys. Data are changes in EEG bandwidth, normalized to percentage of baseline (mean – SEM, $N = 4$). Functions were obtained through non-linear regression analyses using the 4-parameter logistic equation, with minimal effect constrained to 100. The ED_{50} values, shown as mg/kg and SEMs, were significantly different (F test, $p < 0.05$)

0.009). The mean percentage of baseline for the dose of 1.8 mg/kg alprazolam was significantly lower than this mean obtained after vehicle injections (Dunnett's test, $p = 0.048$). For activity (Fig. 4, bottom panel), the repeated measures ANOVA was not significant ($F_{6,18} = 3.57$, $p = 0.08$), but the a priori Dunnett's test showed a significant decrease in the mean percentage of baseline for the dose of 1.8 mg/kg alprazolam compared with the mean obtained with vehicle injections ($p = 0.0018$). As apparent from the figure, there was a trend for a biphasic effect, with the dose of 0.1 mg/kg above 100% of baseline for three of four monkeys. However, removal of monkey M-RQ-6118 from the analysis did not change the pattern of results. Finally, analyses of EMG data revealed no statistically significant effects (data not shown; $F_{6,18} = 0.75$).

In order to determine if the behavioral/physiological measures were correlated with spectral power band alterations following alprazolam injections, Pearson correlations were computed for all doses of alprazolam (minus vehicle) for each significant power band change, as shown in Table 2 (EEG power), Table 3 (normalized power), and Table 4 (normalized relative power). For the non-transformed power data (Table 2), the overall pattern of effects were significant correlations primarily in the central derivation for both body

Fig. 4 Peripheral body temperature (top panel) and activity (bottom panel) following vehicle and doses of alprazolam in rhesus monkeys. Each symbol represents an individual monkey, identified by in the legend. The functions connect to horizontal bars that represent the means for each dose or vehicle (V). Data are percentages of baseline (i.e., in the absence of injections). Multiple comparisons, represented by the bars with $p < 0.05$, were Dunnett's tests

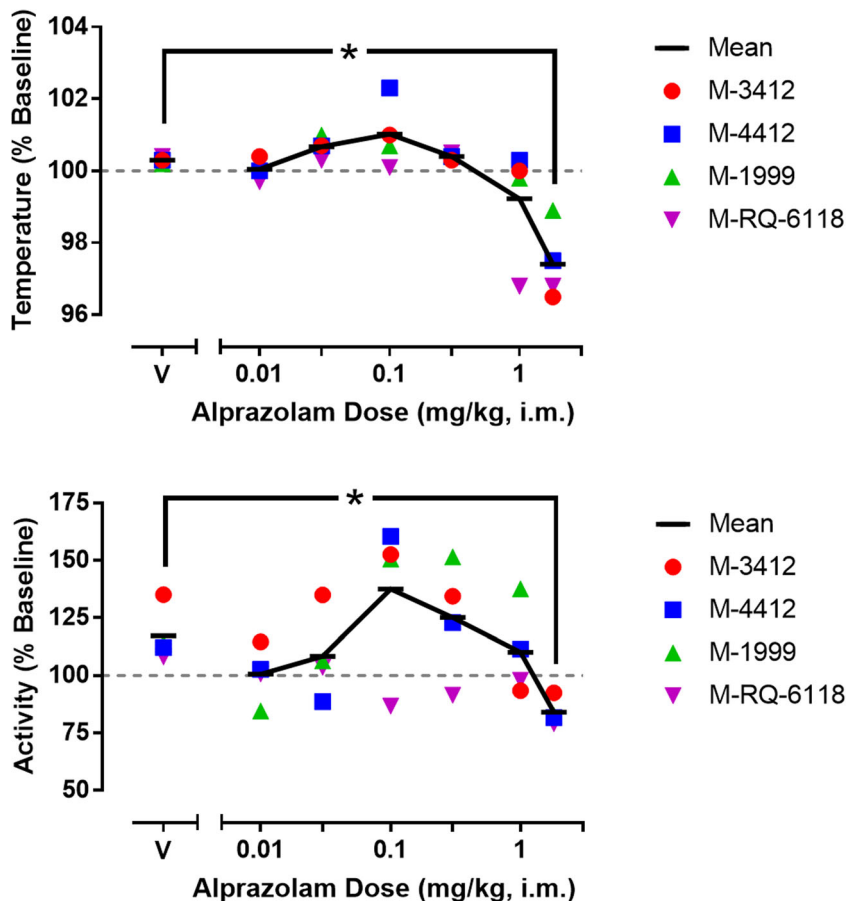


Table 2 Pearson correlation analyses comparing behavioral/physiological effects with spectral power bands as EEG power ($\mu\text{V}^2/\text{Hz}$) following alprazolam administration in rhesus monkeys

Effect	Pearson <i>r</i> <i>p</i> value								
	Delta occipital	Theta occipital	Alpha occipital	Sigma occipital	Beta occipital	Delta central	Theta central	Sigma central	Beta central
Body temperature	−0.988 <i>0.001</i>	−0.144 <i>0.393</i>	0.289 <i>0.290</i>	0.352 <i>0.247</i>	0.044 <i>0.467</i>	−0.974 <i>0.001</i>	−0.972 <i>0.001</i>	−0.969 <i>0.001</i>	−0.910 <i>0.006</i>
Activity	−0.769 <i>0.037</i>	−0.596 <i>0.106</i>	−0.241 <i>0.323</i>	−0.175 <i>0.370</i>	−0.409 <i>0.210</i>	−0.725 <i>0.051</i>	−0.762 <i>0.039</i>	−0.745 <i>0.045</i>	−0.603 <i>0.103</i>

Data are correlations of each power band with 0.01, 0.03, 0.1, 0.3, 1.0, and 1.8 mg/kg (i.m.) of alprazolam for each effect and based on data from $N = 4$ monkeys. Numbers in italics represent *p* values. Blue-shaded areas indicate statistically significant correlations, $p \leq 0.05$

temperature and activity, with only delta frequencies in occipital significant as a function of both body temperature and activity. Relatively strong correlations (*r* values of −0.91 to −0.974) were observed with alprazolam's effects on body temperature and delta, theta, sigma, and beta power frequencies. For activity, significant correlations were observed for both measures with theta and sigma frequencies.

A similar pattern of effects with the correlations was observed when EEG power was normalized to baseline values (Table 3). For this analysis, no significant correlations with either body temperature or activity were observed with spectral power bands in the occipital derivation. In contrast, all power bands in the central derivation showed robust ($r_s > 0.90$) relationships for body temperature, with significant correlations for activity with theta, alpha, and sigma bands. Finally, with the conversion to normalized relative power, significant negative correlations were obtained for decreases in peripheral body temperature with increases in delta bands (occipital derivation), as well as increases in sigma bands (central derivation). For activity, a significant negative correlation was observed for the decrease in activity and increase in sigma bands (central derivation).

Discussion

The present study shows that daytime alprazolam treatment in male rhesus monkeys increased EEG power (including beta activity) overall in central brain regions, while EEG delta power increased and EEG alpha, theta, and sigma power decreased in occipital brain regions in a dose-dependent manner. There was an ~8-fold difference in the potency of alprazolam to increase central EEG beta power vs. occipital EEG delta power (based on relative EEG power), corroborating the assumption that EEG beta band increases are associated with lower, anxiolytic doses, whereas EEG delta band effects are associated with higher, sedative doses of benzodiazepines. Accordingly, a dose of alprazolam that increased central EEG beta band frequency but did not significantly increase EEG delta band frequency (0.3 mg/kg, with the ED_{50} for increasing central EEG beta power being 0.055 mg/kg) did not have sedative effects. On the other hand, the highest dose tested (1.8 mg/kg), which increased both central EEG beta power and occipital relative EEG delta power, significantly increased total sleep time by increasing time spent in N1 and N2 sleep stages. Finally, the highest dose of alprazolam decreased peripheral body temperature and general locomotor activity.

Table 3 Pearson correlation analyses comparing behavioral/physiological effects with spectral power bands as normalized power (% baseline) following alprazolam administration in rhesus monkeys

Effect	Pearson <i>r</i> <i>p</i> value								
	Theta occipital	Alpha occipital	Sigma occipital	Beta occipital	Delta central	Theta central	Alpha central	Sigma central	Beta Central
Body temperature	−0.092 <i>0.431</i>	0.272 <i>0.301</i>	0.317 <i>0.100</i>	0.005 <i>0.496</i>	−0.971 <i>< 0.001</i>	−0.980 <i>< 0.001</i>	−0.983 <i>< 0.001</i>	−0.989 <i>< 0.001</i>	−0.945 <i>0.002</i>
Activity	−0.560 <i>0.124</i>	−0.258 <i>0.311</i>	−0.217 <i>0.340</i>	−0.461 <i>0.178</i>	−0.722 <i>0.053</i>	−0.764 <i>0.039</i>	−0.794 <i>0.030</i>	−0.751 <i>0.043</i>	−0.640 <i>0.086</i>

Data are correlations of each power band with 0.01, 0.03, 0.1, 0.3, 1.0, and 1.8 mg/kg (i.m.) of alprazolam for each effect and based on data from $N = 4$ monkeys. Numbers in italics represent *p* values. Blue-shaded areas indicate statistically significant correlations, $p \leq 0.05$.

Table 4 Pearson correlation analyses comparing behavioral/physiological effects with spectral power bands as normalized relative power (% baseline) following alprazolam administration in rhesus monkeys

Effect	Pearson <i>r</i> <i>p</i> value					
	Delta occipital	Theta occipital	Alpha occipital	Sigma occipital	Sigma central	Beta central
Body temperature	−0.766 <i>0.038</i>	0.635 <i>0.088</i>	0.462 <i>0.178</i>	0.583 <i>0.112</i>	−0.970 <i><0.001</i>	−0.543 <i>0.133</i>
Activity	−0.362 <i>0.241</i>	0.117 <i>0.413</i>	−0.073 <i>0.445</i>	0.087 <i>0.435</i>	−0.775 <i>0.035</i>	−0.090 <i>0.433</i>

Data are correlations of each power band with 0.01, 0.03, 0.1, 0.3, 1.0, and 1.8 mg/kg (i.m.) of alprazolam for each effect and based on data from $N = 4$ monkeys. Numbers in italics represent *p* values. Blue-shaded areas indicate statistically significant correlations, $p \leq 0.05$.

Our findings are in agreement with the human and rodent literature indicating that anxiolytic, non-sedating, doses of benzodiazepines increase EEG beta and sigma power and decrease EEG alpha power (Coenen and van Luijtelaar 1991; Jongsma et al. 2000; van Lier et al. 2004; Saletu et al. 2006; Gilles and Luthringer 2007; Christian et al. 2015). Specifically, acute alprazolam administration has been shown to increase EEG beta and decrease alpha in healthy volunteers (Barbanoj et al. 2007). Although EEG changes, particularly increased EEG beta activity, have been proposed extensively as a quantitative biomarker for GABA_A receptor modulation (Visser et al. 2003), to the best of our knowledge this phenomenon had not been previously demonstrated in adult nonhuman primates (for studies on diazepam-associated cortical laterality based on EEG in infant monkeys, see Davidson et al. 1992, 1993). Also in agreement with previous reports in humans (Buchsbaum et al. 1985; Veselis et al. 1991), EEG activity changes after alprazolam administration followed a topographic distribution, with EEG beta power increasing only in the central derivation. These findings emphasize the importance of multi-lead recording in assessing EEG correlates of benzodiazepine action, particularly recordings including central and occipital EEG derivations.

Topographic distribution also was evident for sedative doses of alprazolam. In this regard, a relatively high dose of alprazolam increased relative EEG delta power, an effect that was restricted to occipital brain regions. The specific EEG power changes observed with sedative doses of alprazolam are in agreement with previous reports in rodents and humans (Schulte am Esch and Kochs 1990; Veselis et al. 1991; Hering et al. 1994; Liu et al. 1996; Schnider et al. 1996). Our findings also corroborate the premise of “pharmacological dissociation” (i.e., the fact that benzodiazepines increase EEG beta band frequency at doses that are also sedative) first proposed by Wikler (1952). In fact, when analyzing raw or normalized raw EEG power, an increase in delta EEG frequency is observed even in central brain regions. Therefore, this concept implies that a quantitative analysis of EEG alone might give

incorrect information about the effects of a compound on the state of vigilance (Coenen and van Luijtelaar 1991).

Nutt et al. (2015) have also shown that, in agreement with our findings, the administration of the benzodiazepine-type drug zolpidem increased EEG beta band frequency in central brain regions and EEG delta band frequency in occipital brain regions in healthy human volunteers. Because zolpidem has selective affinity for GABA_A receptors containing $\alpha 1$ subunits ($\alpha 1$ GABA_A receptors) (Huang et al. 2000), the delta-increasing and consequent sedative effects of benzodiazepine drugs have been proposed to be mediated by $\alpha 1$ GABA_A receptors. On the other hand, growing evidence from the rodent and nonhuman primate literature suggests that GABA_A receptors containing $\alpha 2$ subunits ($\alpha 2$ GABA_A receptors) mediate benzodiazepine-induced anxiolysis (Engin et al. 2018; Meng et al. 2020). Benzodiazepine-type compounds with selective efficacy at GABA_A receptors containing $\alpha 2$ and $\alpha 3$ subunits ($\alpha 2/3$ GABA_A receptors) selectively increase EEG beta and gamma power in rodents, having no effects on EEG delta power (Christian et al. 2015). Moreover, compounds with selectivity for $\alpha 2/3$ GABA_A receptors only induce mild sedative effects (rest/sleep posture, i.e., idiosyncratic posture adopted by monkeys during rest or sleep, easily roused) at high doses in behavioral observation studies in rhesus monkeys (Duke et al. 2018). Collectively, these findings suggest that $\alpha 1$ GABA_A receptors mediate benzodiazepine-induced sedation and increased EEG delta activity, while $\alpha 2$ GABA_A mediate benzodiazepine-induced anxiolysis and increase EEG beta activity, although additional research is needed to explore this hypothesis in primate species.

Although no studies have reported effects of benzodiazepines on EEG activity during the wake cycle in adult monkeys, at least two studies examined the effects of benzodiazepine-type drugs during the sleep cycle with fully implantable telemetry systems. Tannenbaum et al. (2016) showed that administration of eszopiclone or diazepam 2 h before “lights off” in rhesus monkeys decreased delta/slow-wave sleep and REM sleep while increasing light sleep

compared to vehicle. Authier et al. (2014) investigated EEG power changes during the nighttime after acute administration of diazepam in cynomolgus monkeys. In agreement with the sleep data observed in the present study, the authors report a slight (although not statistically significant) increase in duration of N2 sleep stage compared to a baseline night of sleep (Authier et al. 2014). Of note, the main effect observed after diazepam treatment was a significant decrease in EEG power activity in low frequencies (spectral power between 1 and 13 Hz, equivalent to delta, theta, and alpha activity) during all vigilance states, as well as an increase in EEG activity in high frequencies (spectral power above 30 Hz, equivalent to beta activity) during sleep (Authier et al. 2014). Although the findings showing EEG beta power increase and EEG theta power decrease are in agreement with our findings, the EEG delta activity changes observed by Authier et al. (2014) are the opposite of those reported in the present study. Therefore, specific daytime vs. nighttime differences might be observed on EEG activity after administration of benzodiazepine drugs in primates. Of note, in their study, Authier et al. (2014) used a single EEG lead for their recordings according to a standard bipolar derivation: Cz–Oz (central–occipital) (Authier et al. 2014). Therefore, the authors were not able to capture topographical (central vs. occipital) EEG changes, as shown in the present study, which could also have contributed to the differences observed between the two studies.

Daytime alprazolam administration also decreased peripheral body temperature at the highest dose tested. Benzodiazepine-induced hypothermia has been previously reported in rodents (Taylor et al. 1985; Jackson and Nutt 1990, 1991), humans (Hostler et al. 2009) and macaques (cynomolgus monkeys; Moscardo et al. 2010). The highest dose of alprazolam also significantly decreased general home-cage locomotor activity, which is in agreement with its sedative effects (NREM sleep-inducing effects and increased EEG delta power). Interestingly, peripheral body temperature was negatively correlated with central EEG activity, particularly for raw and normalized raw EEG power. It is well known that sleep in mammals is accompanied by a decrease in core body temperature (Szymusiak 2018). Because in the present study sleep–wake state scoring was conducted based on recordings from the central derivation, it is possible that the correlations between body temperature and EEG power were a result of a decrease in core body temperature specifically during sleep. Although the relationship between sleep EEG power and changes in body temperature remains unknown, the neural control of sleep and thermoregulation anatomically and functionally overlap within the preoptic/anterior hypothalamus (for review, see Szymusiak 2018).

Interestingly, NREM EEG sigma power is an important correlate of spindle density (Wamsley et al. 2012). Sleep spindles are a defining EEG oscillation of N2 sleep stages and are characterized as brief bursts of 12–15-Hz activity (Berry et al. 2018). Spindles

are the product of a thalamocortical feedback loop that is regulated by GABAergic receptors located in the thalamic reticular nucleus and have been proposed as key facilitators of synaptic plasticity involved in memory consolidation (for review, see Manoach et al. 2016). Benzodiazepines are known to increase spindle density in healthy human volunteers (Azumi and Shirakawa 1982; Suetsugu et al. 2001; Plante et al. 2015), and increasing spindles with acute administration of zolpidem (Kaestner et al. 2013; Mednick et al. 2013) has been shown to improve memory, whereas transcranial stimulation that decreases EEG sigma power impairs memory (Marshall et al. 2011). However, long-term benzodiazepine use induces memory deficits (Crowe and Stranks 2018). Further studies are needed to systematically investigate the effects of acute and chronic benzodiazepine drugs on sleep spindles in primates and identify their correlates.

In summary, our study is the first to demonstrate that a benzodiazepine drug induced a signature dose-dependent EEG change in nonhuman primates. This effect was similar to what has been previously reported in rodents and humans, both at doses expected to exert anxiolytic-related effects, as well as higher, sedative doses. We also show that a highly translational species shows the same topography-dependent pattern of effects on EEG power spectrum with benzodiazepine treatment as seen in humans. Finally, daytime alprazolam administration in rhesus monkeys induced other translationally relevant effects, including decreased body temperature and increased EEG sigma power, a correlate of spindle density. The present study shows that EEG power can be used to evaluate benzodiazepine effects in rhesus monkeys and provides a valuable model for studying benzodiazepine pharmacology.

Acknowledgments The authors thank Megan Fine and Vince Mendenhall for their surgical services and guidance during the animal recovery period. We also thank Troy Velie and Lorie Boyd for assistance with the use of DSI hardware and software. The authors thank Megan Follett and Joseph Talley for technical assistance and Chris Young for assistance with data analysis. Finally, we thank the veterinary staff from the UMMC Center for Comparative Research for their valuable help during the establishment of this model/procedure and for their constant care for our animals.

Author contributions LFB and JKR were responsible for the study concept and design. LFB and JRD contributed to the acquisition of data. LFB, JSO, and JKR assisted with data analysis and interpretation of findings. LFB and JKR drafted the manuscript. All authors read and provided critical revision of the manuscript for important intellectual content and approved the final version for publication.

Funding This work was supported by the National Institutes of Health (DA011792, DA043204, DA046778, and DA049886).

Declarations

Conflict of interest No conflict declared.

References

- Algina J, Olejnik S (2003) Conducting power analyses for ANOVA and ANCOVA in between-subjects designs. *Eval Health Prof* 26:288–314
- Authier S, Bassett L, Pouliot M, Rachalski A, Troncy E, Paquette D, Mongrain V (2014) Effects of amphetamine, diazepam and caffeine on polysomnography (EEG, EMG, EOG)-derived variables measured using telemetry in Cynomolgus monkeys. *J Pharmacol Toxicol Methods* 70:86–93
- Azumi K, Shirakawa S (1982) Characteristics of spindle activity and their use in evaluation of hypnotics. *Sleep* 5:95–105
- Bachhuber MA, Hennessy S, Cunningham CO, Starrels JL (2016) Increasing benzodiazepine prescriptions and overdose mortality in the United States, 1996–2013. *Am J Public Health* 106:686–688
- Bakeman R (2005) Recommended effect size statistics for repeated measures designs. *Behav Res Methods* 37:379–384
- Barbanj MJ, Urbano G, Antonijoan R, Ballester MR, Valle M (2007) Different acute tolerance development to EEG, psychomotor performance and subjective assessment effects after two intermittent oral doses of alprazolam in healthy volunteers. *Neuropsychobiology* 55:203–212
- Berry RB, Albertario CL, Harding SM, Lloyd RM, Plante DT, Quan SF, Troester MM, Vaughn BV, for the American Academy of Sleep Medicine (2018) The AASM manual for the scoring of sleep and associated events: rules, terminology and technical specifications. Version 2.5. American Academy of Sleep Medicine, Darien, IL
- Brown RE, Basheer R, McKenna JT, Strecker RE, McCarley RW (2012) Control of sleep and wakefulness. *Physiol Rev* 92:1087–1187
- Buchsbaum MS, Hazlett E, Sicotte N, Stein M, Wu J, Zetin M (1985) Topographic EEG changes with benzodiazepine administration in generalized anxiety disorder. *Biol Psychiatry* 20:832–842
- Christian EP, Snyder DH, Song W, Gurley DA, Smolka J, Maier DL, Ding M, Gharahdaghi F, Liu XF, Chopra M, Ribadeneira M, Chapdelaine MJ, Dudley A, Arriza JL, Maciag C, Quirk MC, Doherty JJ (2015) EEG- β/γ spectral power elevation in rat: a translatable biomarker elicited by GABA(A α 2/3)-positive allosteric modulators at non-sedating anxiolytic doses. *J Neurophysiol* 113:116–131
- Coenen AM, van Luijckelaar EL (1991) Pharmacological dissociation of EEG and behavior: a basic problem in sleep-wake classification. *Sleep* 14:464–465
- Crowe SF, Stranks EK (2018) The residual medium and long-term cognitive effects of benzodiazepine use: an updated meta-analysis. *Arch Clin Neuropsychol* 33:901–911
- Davidson RJ, Kalin NH, Shelton SE (1992) Lateralized effects of diazepam on frontal brain electrical asymmetries in rhesus monkeys. *Biol Psychiatry* 32:438–451
- Davidson RJ, Kalin NH, Shelton SE (1993) Lateralized response to diazepam predicts temperamental style in rhesus monkeys. *Behav Neurosci* 107:1106–1110
- Duke AN, Meng Z, Platt DM, Atack JR, Dawson GR, Reynolds DS, Tiruveedhula VVNPB, Li G, Stephen MR, Sieghart W, Cook JM, Rowlett JK (2018) Evidence that sedative effects of benzodiazepines involve unexpected GABA_A receptor subtypes: quantitative observation studies in rhesus monkeys. *J Pharmacol Exp Ther* 366:145–157
- Engin E, Benham RS, Rudolph U (2018) An emerging circuit pharmacology of GABA_A receptors. *Trends Pharmacol Sci* 39:710–732
- Gilles C, Luthringer R (2007) Pharmacological models in healthy volunteers: their use in the clinical development of psychotropic drugs. *J Psychopharmacol (Oxf)* 21:272–282
- Goonawardena AV, Morairty SR, Orellana GA, Willoughby AR, Wallace TL, Kilduff TS (2018) Electrophysiological characterization of sleep/wake, activity and the response to caffeine in adult cynomolgus macaques. *Neurobiol Sleep Circadian Rhythms* 6:9–23
- Hering W, Geisslinger G, Kamp HD, Dinkel M, Tschakowsky K, Rügheimer E, Brune K (1994) Changes in the EEG power spectrum after midazolam anaesthesia combined with racemic or S- (+) ketamine. *Acta Anaesthesiol Scand* 38:719–723
- Hostler D, Northington WE, Callaway CW (2009) High-dose diazepam facilitates core cooling during cold saline infusion in healthy volunteers. *Appl Physiol Nutr Metab* 34:582–586
- Hsieh KC, Robinson EL, Fuller CA (2008) Sleep architecture in unrestrained rhesus monkeys (*Macaca mulatta*) synchronized to 24-hour light-dark cycles. *Sleep* 31:1239–1250
- Huang Q, He X, Ma C, Liu R, Yu S, Dayer CA, Wenger GR, McKernan R, Cook JM (2000) Pharmacophore/receptor models for GABA(A)/BzR subtypes (alpha1beta3gamma2, alpha5beta3gamma2, and alpha6beta3gamma2) via a comprehensive ligand-mapping approach. *J Med Chem* 43:71–95
- Jackson HC, Nutt DJ (1990) Body temperature discriminates between full and partial benzodiazepine receptor agonists. *Eur J Pharmacol* 185:243–246
- Jackson HC, Nutt DJ (1991) Comparison of the effects of benzodiazepine and beta-carboline inverse agonists on body temperature in mice. *Eur J Pharmacol* 205:213–216
- Jongsma ML, van Rijn CM, van Egmond J, van Schaijk WJ, Sambeth A, Coenen AM (2000) The influence of diazepam on the electroencephalogram-evoked potential interrelation in rats. *Neurosci Lett* 293:83–86
- Kaestner EJ, Wixted JT, Mednick SC (2013) Pharmacologically increasing sleep spindles enhances recognition for negative and high-arousal memories. *J Cogn Neurosci* 25:1597–1610
- Leiser SC, Dunlop J, Bowlby MR, Devillbliss DM (2011) Aligning strategies for using EEG as a surrogate biomarker: a review of preclinical and clinical research. *Biochem Pharmacol* 81:1408–1421
- Liu J, Singh H, White PF (1996) Electroencephalogram bispectral analysis predicts the depth of midazolam-induced sedation. *Anesthesiology* 84:64–69
- Manoach DS, Pan JQ, Purcell SM, Stickgold R (2016) Reduced sleep spindles in schizophrenia: a treatable endophenotype that links risk genes to impaired cognition? *Biol Psychiatry* 80:599–608
- Marshall L, Kirov R, Brade J, Molle M, Born J (2011) Transcranial electrical currents to probe EEG brain rhythms and memory consolidation during sleep in humans. *PLoS One* 6:e16905
- Mednick SC, McDevitt EA, Walsh JK, Wamsley E, Paulus M, Kanady JC, Drummond SPA (2013) The critical role of sleep spindles in hippocampal-dependent memory: a pharmacology study. *J Neurosci* 33:4494–4504
- Meng Z, Berro LF, Sawyer EK, Rüedi-Bettschen D, Cook JE, Li G, Platt DM, Cook JM, Rowlett JK (2020) Evaluation of the anti-conflict, reinforcing, and sedative effects of YT-III-31, a ligand functionally selective for α 3 subunit-containing GABA_A receptors. *J Psychopharmacol* 34:348–357
- Möhler H (2011) The rise of a new GABA pharmacology. *Neuropharmacology* 60:1042–1049
- Moore TJ, Mattison DR (2017) Adult utilization of psychiatric drugs and differences by sex, age, and race. *JAMA Intern Med* 177:274–275
- Moscato E, McPhie G, Fasdelli N, Giarola A, Tontodonati M, Dorigatti R, Meecham K (2010) An integrated cardiovascular and neurobehavioural functional assessment in the conscious telemetered cynomolgus monkey. *J Pharmacol Toxicol Methods* 62:95–106
- Myers JL, Well AD, Lorch RF Jr (2010) Research design and statistical analysis: third edition. Routledge, New York, NY
- National Research Council (2011) Guide for the care and use of laboratory animals, 8th edn. The National Academies Press, Washington, DC

- Nishida M, Zestos MM, Asano E (2016) Spatial-temporal patterns of electrocorticographic spectral changes during midazolam sedation. *Clin Neurophysiol* 127:1223–1232
- Nutt D, Wilson S, Lingford-Hughes A, Myers J, Papadopoulos A, Muthukumaraswamy S (2015) Differences between magnetoencephalographic (MEG) spectral profiles of drugs acting on GABA at synaptic and extrasynaptic sites: a study in healthy volunteers. *Neuropharmacology* 88:155–163
- Plante DT, Goldstein MR, Cook JD, Smith R, Riedner BA, Rumble ME, Jelenchick L, Roth A, Tononi G, Benca RM, Peterson MJ (2015) Effects of oral temazepam on sleep spindles during non-rapid eye movement sleep: a high-density EEG investigation. *Eur Neuropsychopharmacol* 25:1600–1610
- Rowlett JK, Lelas S, Tomatzky W, Licata SC (2006) Anti-conflict effects of benzodiazepines in rhesus monkeys: relationship with therapeutic doses in humans and role of GABA_A receptors. *Psychopharmacology (Berl)* 184:201–211
- Ruehland WR, O'Donoghue FJ, Pierce RJ, Thornton AT, Singh P, Copland JM, Stevens B, Rochford PD (2011) The 2007 AASM recommendations for EEG electrode placement in polysomnography: impact on sleep and cortical arousal scoring. *Sleep* 34:73–81
- Saletu B, Anderer P, Saletu-Zyhlarz GM (2006) EEG topography and tomography (LORETA) in the classification and evaluation of the pharmacodynamics of psychotropic drugs. *Clin EEG Neurosci* 37:66–80
- Santo L, Rui P, Ashman JJ (2020) Physician office visits at which benzodiazepines were prescribed: findings from 2014 to 2016 National Ambulatory Medical Care Survey. *Natl Health Stat Report* 137:1–16
- Schnider TW, Minto CF, Fiset P, Gregg KM, Shafer SL (1996) Semilinear canonical correlation applied to the measurement of the electroencephalographic effects of midazolam and flumazenil reversal. *Anesthesiology* 84:510–519
- Schulte am Esch J, Kochs E (1990) Midazolam and flumazenil in neuroanaesthesia. *Acta Anaesthesiol Scand Suppl* 92:96–102
- Sperk G, Kirchmair E, Bakker J, Sieghart W, Drexel M, Kondova I (2020) Immunohistochemical distribution of 10 GABA_A receptor subunits in the forebrain of the rhesus monkey *Macaca mulatta*. *J Comp Neurol* 528:2551–2568
- Suetsugi M, Mizuki Y, Ushijima I, Kobayashi T, Watanabe Y (2001) The effects of diazepam on sleep spindles: a qualitative and quantitative analysis. *Neuropsychobiology* 43:49–53
- Szymusiak R (2018) Body temperature and sleep. *Handb Clin Neurol* 156:341–351
- Tallon-Baudry C, Mandon S, Freiwald WA, Kreiter AK (2004) Oscillatory synchrony in the monkey temporal lobe correlates with performance in a visual short-term memory task. *Cereb Cortex* 14:713–720
- Tannenbaum PL, Tye SJ, Stevens J, Gotter AL, Fox SV, Savitz AT, Coleman PJ, Uslaner JM, Kuduk SD, Hargreaves R, Winrow CJ, Renger JJ (2016) Inhibition of orexin signaling promotes sleep yet preserves salient arousability in monkeys. *Sleep* 39:603–612
- Taylor SC, Little HJ, Nutt DJ, Sellars N (1985) A benzodiazepine agonist and contragonist have hypothermic effects in rodents. *Neuropharmacology* 24:69–73
- van Lier H, Drinkenburg WH, van Eeten YJ, Coenen AM (2004) Effects of diazepam and zolpidem on EEG beta frequencies are behavior-specific in rats. *Neuropharmacology* 47:163–174
- Veselis RA, Reinsel R, Sommer S, Carlon G (1991) Use of neural network analysis to classify electroencephalographic patterns against depth of midazolam sedation in intensive care unit patients. *J Clin Monit* 7:259–267
- Visser SAG, Wolters FLC, Gubbens-Stibbe JM, Tukker E, Van der Graaf PH, Peletier LA, Danhof M (2003) Mechanism-based PK/PD modelling of the EEG effects of GABAA receptor modulators: in vitro/in vivo correlations. *J Pharmacol Exp Ther* 304:88–101
- Votaw VR, Geyer R, Rieselbach MM, McHugh RK (2019) The epidemiology of benzodiazepine misuse: a systematic review. *Drug Alcohol Depend* 200:95–114
- Wamsley E, Tucker MA, Shinn AK, Ono KE, McKinley S, Ely AV, Goff DC, Stickgold R, Manoach DS (2012) Reduced sleep spindles and spindle coherence in schizophrenia: mechanisms of impaired memory consolidation? *Biol Psychiatry* 71:154–161
- Wikler A (1952) Pharmacologic Dissociation of Behavior and EEG "Sleep Patterns" in Dogs: Morphine, N-Allylnormorphine, and Atropine. *Proc Soc Exp Biol NY* 79:261–265

Publisher's note Springer Nature remains neutral with regard to jurisdictional claims in published maps and institutional affiliations.